Quantum Transport Calculations Using Periodic Boundary Conditions

Lin-Wang Wang
Computational Research Division, Lawrence Berkeley National Laboratory, Berkeley, CA 94720
(Dated: June 14, 2004)

An efficient new method is presented to calculate the quantum transports using periodic boundary conditions. This method allows the use of conventional ground state ab initio programs without big changes. The computational effort is only a few times of a normal ground state calculation, thus it makes accurate quantum transport calculations for large systems possible.

PACS numbers: 71.15.-m, 73.63.-b, 73.22.-f

Quantum transport for molecules, nanowires, and nanodevices is a fast growing research area in both experiment and theory, with the potential of replacing the current Si based technology after the Moor's law reaches its limit in about 15 years. In the theoretical ballistic transport calculations, a key step is to calculate the current via the Landauer formula:

$$I = \frac{2e}{h} \int_{\mu_L}^{\mu_R} \sum_n T_n(E) dE, \tag{1}$$

where μ_L and μ_R are left and right electrode Fermi energies (assuming the current flows from right to left in z direction), and $T_n(E)$ is the transmission coefficient for the nth right hand electrode channel (band) at energy E. There are two major ways to calculate $T_n(E)$. One is to use the Green's function $G(\mathbf{r}, \mathbf{r}', E)$ of the system. However since G is a double variable function, computationally this approach can be quite expensive, thus it is mostly used for localized basis set methods [1]. The other way to calculate $T_n(E)$ is to solve the following scattering states:

$$H\psi_{sc}(r) = E\psi_{sc}(r) \tag{2}$$

and for $z \to \infty(-\infty)$:

$$\psi_{sc}(r) = \sum_n [A_n^{R(L)} \phi_n^{R(L)*}(r) + B_n^{R(L)} \phi_n^{R(L)}(r)], \tag{3}$$

with conditions: $A_n^R = 0$ except $A_m^R = 1$ for one m, and $B_n^L = 0$ (assuming $dE_n^{R(L)}(k)/dk > 0$). In above, H is the single particle Hamiltonian, and $\phi_n^{R(L)}(r) = u_{n,k_n}(r) exp(ik_n^{R(L)} z)$ are right going running waves in the the right(R) and left(L) electrodes, and $\phi_n^{R(L)*}$ are the left going running waves. $E_n^{R(L)}(k_n^{R(L)}) = E$ are the electrode band structure. The transmission coefficient for channel m can be calculated as $T_m(E) = [\sum_n |A_n^L|^2 (dE_n^L(k)/dk)]/(dE_m^R(k)/dk)$, and the reflection coefficient can be calculated as $R_m(E) = [\sum_n |B_n^R|^2 (dE_n^R(k)/dk)]/(dE_m^R(k)/dk)$. Transfer matrix method [2, 3] and the Lippmann-Schwinger equation [5] have been used to solve Eqs(2),(3). Unfortunately, the transfer matrix method is rather complicated and computationally expensive to deal with the nonlocal pseudopotentials [3] and it is often plagued by the numerical instability due to the evanescent states in a multi-channel electrode [4]. On the other hand, the use of Lippmann-Schwinger equation [5] requires the solution of a linear equation of the dimension of the full system, and it also needs the Green's function of the two electrode system under a potential bias. As a result, currently this approach is only used for jellium electrode model and relatively small systems. Overall, compared to the more matured ground state calculations, all the current methods for transport calculations are complicated and computationally expensive, and they can only be used to calculate relatively small systems although there is a strong need to study the transports of large molecules and nanostructures. Here, we present a new and simple approach which makes the transport calculation similar to the ground state calculation. In this approach, conventional periodic supercell methods and a specially designed perturbative approach are used to solve Eqs(2),(3). This allows us to use modern ab initio total energy programs without much change. The computational effort is similar to a normal ground state local density approximation (LDA) calculation, hence it opens the door for quantum transport studies for large systems.

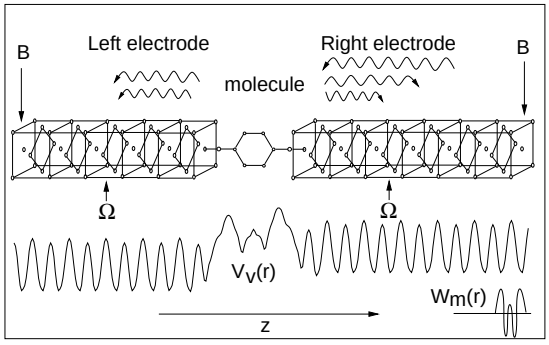

FIG. 1: A schematic view of the calculated system.

To demonstrate our method, we have chosen a benzene molecule connected by two Cu quantum wires as shown in Fig.1. This system is chosen since the conductivity of the benzene molecule is well studied [5, 6] and similar

quantum wires have been used as electrodes in previous quantum transport calculations [7]. Two hydrogen atoms at the two ends of the benzene molecule are replaced by two sulfur atoms, which are bonded to two central Cu atoms at the electrode. The atomic positions of the molecule are relaxed at the zero voltage bias under LDA calculation. We have used norm conserving pseudopotentials and 30 Ryd planewave cutoff with a standard planewave LDA program [8]. We have included 5 and 6 unit cells in the left and right electrodes respectively, and they are connected at boundary B in Fig.1 by periodic boundary condition. The x, y dimensions of the supercell are 3 times the width of the Cu wire to avoid possible neighbore-neighbore interactions. After the Kohn-Sham single particle potential $V_0(r)$ is obtained from a LDA selfconsistent calculation at the zero bias, we have added a potential $V/2 sin(\pi z/L')$ in the central region of the molecule and shifted the rest of the right (left) electrode by $V/2$ ($-V/2$) to get the potential $V_V(r)$ for a bias V system. Although a selfconsistent treatment can be achieved straight forwardly under the current approach [since the scattering states of Eq(2) will be calculated], the current nonselfconsistent treatment for finite bias V is sufficient in illustrating the new methodology. Note that, there is a jump of $V_V(r)$ at the boundary B, but that is not a problem in our numerical calculations.

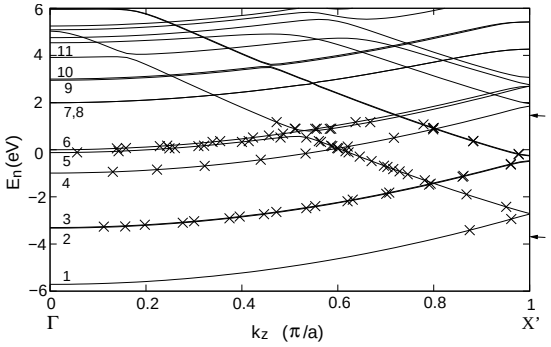

FIG. 2: The band structure of the electrode. Each continuous line from Γ to X' is denoted as one band. The zero is the electrode Fermi energy. The crosses are the k_n^R points, see text for details.

Figure 2 shows the band structures $E_n(k_z)$ of the quantum wire electrode. There are 9 Cu atoms in each unit cell of the electrode. To simplify our calculation and analysis, we did not include the 3d electrons in our pseudopotential. Although this will introduce a significant error in the electrode total energy, the electronic structure near the Fermi surface and the related transport properties are intact. However, for bias larger than 2 V, our electrode should be considered as a model electrode due to the lack of Cu 3d electrons.

To solve the scattering states of Eqs(2),(3), we first calculate the eigenstates $\{\psi_i(r),\ E_i\}$ of the periodic supercell under $V_V(r)$ with a $\mathbf{K}_z$ point (e.g, $\mathbf{K}_z = \pi/2L_z$, where L_z is the length of the supercell and this $\mathbf{K}_z$ is not the k_z of the electrode as in Fig.2) using our standard LDA program [8]. Let's first assume that, using some methods, we can generate l degenerated states $\psi_{i,(l)}(r)$ they all satisfy the Schrodinger's equation $H\psi_{i,(l)} = E_i\psi_{i,(l)}$ (however, for our purpose, this equation needs only to be satisfied within the interior of the supercell, not near the boundary B of Fig.1). The idea is to use a linear combination of these states to construct the scattering states of Eq(2). First, within the R(L) electrode, $\psi_{i,(l)}(r)$ can be decomposed into the electrode states $\phi_n^{R(L)}(r)$ just as in Eq(3). From a given E_i, the available n and $k_n^{R(L)}$ can be found from Fig.2, or say: $E_n(k_n^{R(L)}) + \mu_{R(L)} = E_i$. The corresponding $\phi_n^{R(L)}$ is then generated by numerical interpolations from pre-calculated electrode states. The expansion coefficients $A_n^{R(L)}(i,l)$, $B_n^{R(L)}(i,l)$ for wavefunction $\psi_{i,(l)}$ can be easily calculated from the functional products like: $\int_\Omega \psi_{i,(l)}\phi_n^* d^3r$ and $\int_\Omega \phi_m\phi_n^* d^3r$, where Ω is one electrode unit cell at the middle of the electrodes as shown in Fig.1. We found that, after including the possible evanescent states [9], this expansion typically captures more than 99.99% of the weight of the original $\psi_{i,(l)}$. The next step is to make a linear combination of $\psi_{i,(l)}$ to get the scattering state $\psi_{i,sc}$ of Eq(2):

$$\begin{aligned}\psi_{i,sc} &= \sum_l C_l\psi_{i,(l)} \qquad (4)\\ &= \sum_n\sum_l [C_l A_n^{R(L)}(i,l)\phi_n^*(r) + C_l B_n^{R(L)}(i,l)\phi_n(r)],\end{aligned}$$

here the second equation and the R and L are for r within the right and left electrodes respectively. Note that, due to the use of supercell $\mathbf{K}_z$ point and both ψ_i and ψ_i^* are used as $\psi_{i,(l)}$, $\psi_{i,sc}$ is no longer periodic at the supercell boundary B. To make $\psi_{i,sc}$ in Eq(4) as one scattering state of Eq(3), we need to make it satisfy the boundary conditions of Eq(3):$A^R_{n\neq m} = 0$, $B_n^L = 0$, by selecting C_l. In order to have a solution for C_l, we need N independent $\psi_{i,(l)}$ ($l = 1, N$), if there are N nonzero contributing electrode states n in Eq(4) [counting both the left and right electrodes, but ϕ_n and ϕ_n^* are counted as one].

Notice that, since both $\psi_i(r)$ and $\psi_i^*(r)$ satisfy the Schrodinger's equation $H\psi = E_i\psi$, for systems with only a single channel (N=2), the eigen state $\psi_i(r)$ itself is enough to construct the scattering states $\psi_{i,sc}$ from Eq(4). So, the main task here is for multi-channel cases. In our example, from Fig.2 we see that for a given energy E_i, we could have 4-5 channels. To get the N degenerated $\psi_{i,(l)}$, we will use a perturbative approach. First, we will construct $W_m(r) = u_{m,\Gamma}(r)$ (the $k = 0$ mth electrode state) when z is within the last unit cell of the right electrode near boundary B of Fig.1, and $W_m(r) = 0$ for all the other z (see Fig.1). We will add $\beta|W_m >< W_m|$ as a perturbation in the original H, and solve the following eigenstate equation using our standard LDA program (e.g, using conjugate gradient method):

$$H\psi'_{i,m} + \beta < W_m|\psi'_{i,m} > W_m = (E_i + \Delta E_{i,m})\psi'_{i,m}. \quad (5)$$

Here β is a very small number, hence $\Delta E_{i,m}$ and $\Delta\psi_{i,m} \equiv \psi'_{i,m} - \psi_i$ are both small. Suppose we have solved the above equations for two different m's: m_1 and m_2. Then we can construct $\psi_{i,(l)} = F_1\Delta\psi_{i,m_1} + F_2\Delta\psi_{i,m_2}$, with $F_1\Delta E_{i,m_1} + F_2\Delta E_{i,m_2} = 0$. After dropping the second order terms $\Delta E_{i,m_{1,2}}\Delta\psi_{i,m_{1,2}}$ we have:

$$H\psi_{i,(l)} + \beta \sum_{j=1,2} F_j < W_{m_j}|\psi'_{i,m_j} > W_{m_j} = E_i\psi_{i,(l)} \quad (6)$$

Notice that the W_{m_j} terms are nonzero only near the boundary B, so for all the other places, we have $H\psi_{i,(l)} = E_i\psi_{i,(l)}$. Thus, $\psi_{i,(l)}$ are the wavefunctions we needed. In the simple cases, when there are N total electrode states $\phi_n^{R(L)}$ with nonzero components in the expansion of $\psi_i(r)$ in Eq(4), there will be N/2 right electrode states ϕ_n^R. Then the perturbations by the related N/2 W_m states (which have the same characteristics and cross section symmetries as ϕ_n^R) will introduce N/2 indepedent perturbative wavefunction changes $\Delta\psi_{i,m}$. These $\Delta\psi_{i,m}$ will generate $(N/2-1)$ independent $\psi_{i,(l)}$ states (besides the original ψ_i). Thus, the total number of $\psi_{i,(l)}$ states (counting also $\psi^*_{i,(l)}$) is just N, the exact number we need to construct the scattering state $\psi_{i,sc}$ from Eq(4). This argument remains true when there are evanescent states or the number of electrode states in the left and right electrodes are not the same. Thus, using this procedure, we are guaranteed that there will be enough $\psi_{i,(l)}$ states for a given ψ_i to generate a few corresponding scattering states $\psi_{i,sc}$.

From the supercell eigenstates $\{\psi_i(r), E_i\}$, we can generate a set of $\{k_n^R\}$ from $E_n(k_n^R) + \mu_R = E_i$. These $\{k_n^R\}$ are shown in Fig.2 as the crosses for a 1V bias case (using all the $\psi_i(r)$ with E_i between the two horizontal arrows in Fig.2). As can be described by a phase accumulation model[10], on each band, these k_n^R have roughly equal distances and their total number roughly equals the number of electrode unit cells. We have typically used 6 Γ point electrode states as W_m in Eq(5) starting from the lowest band as annotated in Fig.2. This means we have to solve $\{\psi'_{i,m}\}$ of Eq(5) 6 times using $\{\psi_i\}$ as the initial wavefunctions (Notice that, this number 6 is roughly the number of channels in the problem. The same prefactor is needed in the calculations of other methods like the transfer matrix or Lippmann-Schwinger equation). After $\{\psi'_{i,m}\}$ are calculated, using Eq(4), we can construct a scattering state from each of these k_n^R shown in Fig.2. Two of these constructed scattering states are shown in Fig.3. Notice that the dash lines are $\sum_l C_l\psi_{i,(l)}$ of Eq(4), while the solid lines are the electrode state decompositions [the second line of the Eq(4)]. Within the electrode, the electrode state decomposition gives a very accurate description of the total wavefunction. From these scattering states, the transmission coefficients $T_m(E_i)$ can be calculated, and are shown in Fig.4 as the symbols. The calculated $T_m(E_i) + R_m(E_i)$ is typically very close to 1, indicating the numerical stability of the current method.

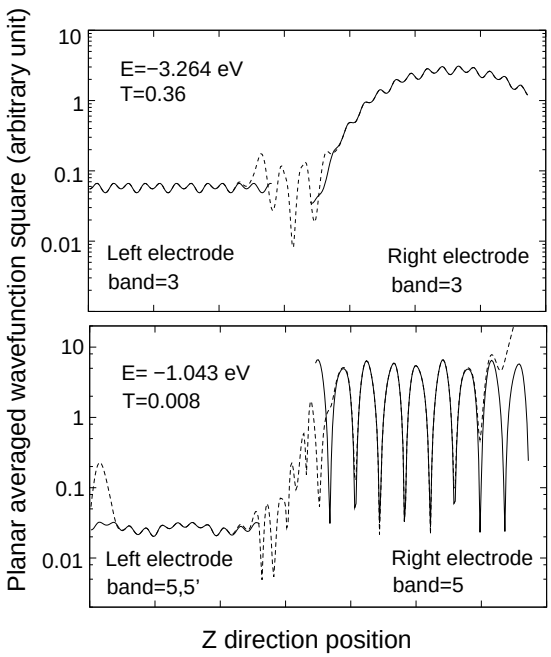

FIG. 3: The constructed scattering states from Eq(4). The dashed and solid lines correspond to the first and second lines of Eq(4) respectively. T is the transmission coefficient, E is the eigen energy, and band number indicate the n of ϕ_n in Eq(4). The bias of the system is 1V.

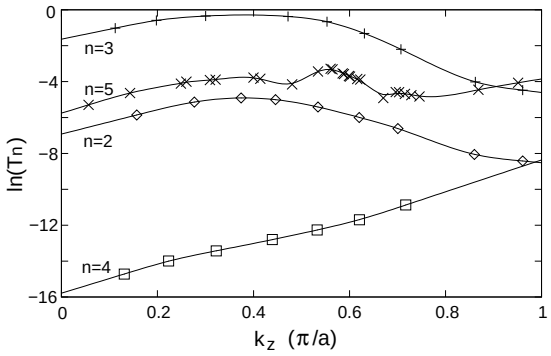

FIG. 4: The calculated transmission coefficients $T_n(k_n^R)$ (symbols) and fitted smooth curves $f_n(k)$ (lines) for different bands of the electrode. The bias of the system is 1V.

Notice that, unlike the other approaches discussed before where the scattering states of arbitrary energy E can be solved, here only the scattering states of energy $\{E_i\}$ are calculated. This translates into finite number of $\{k_n^R\}$ points as shown in Fig.2 and Fig.4. In Eq(1), we need all the energies between μ_L and μ_R. This is an complete analogy with the k-point integration problem in conventional ground state bulk calculation [the energy integral in Eq(1) can also be changed into a k-point integral of the electrode band structure of Fig.2]. Thus, similar to the conventional bulk calculations, here

we will use an interpolation scheme to carry out the integral in Eq(1). First, if the number of $\{k_n^R\}$ is not enough in Fig.4, we can choose a different supercell $\mathbf{K}_z$ in our supercell calculations (or change the potential $V_V(r)$ near boundary B), and repeat the above procedure. That will give us more $\{E_i\}$ and $\{k_n^R\}$ points. In our system, we find one $\mathbf{K}_z$ calculation is sufficient. We have used a smooth curve $f_n(k)$ to interpolate the $ln(T_n(k_n^R))$ points shown in Fig.4. More specifically, we have minimized: $\sum_{k_n^R} |ln(T_n(k_n^R)) - f_n(k_n^R)|^2 + \gamma \int |d^2 f_n(k)/dk^2|^2 dk$, with $\gamma \sim 1$. Numerically, this corresponds to a simple linear equation with discretized k points. The resulting curve is shown in Fig.4 for the 1V bias case. Using these $f_n(k)$, we can calculate the total transmission $T(E) = \sum_n T_n(E)$ of the system. The results are shown in Fig.5 for different biases. We see that $T(E)$ is influenced strongly by two factors. One is the relative energy levels between the electrode states and the molecule states. When the bias increases, the molecular levels drop relative to the right electrode state levels. As a result, the magnitude of the transmission decreases near the region of -3 eV. Another factor is the band structure of the electrode. There is a well shape of $T(E)$ near -0.3 eV. This is caused by band gaps of the 2,3 bands at the X' point in Fig.2. The $T(E)$ also shows a big drop at -3.3 eV. This is due to the end of 2,3 bands at the Γ point.

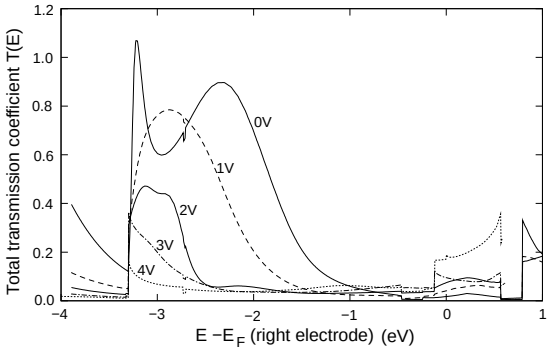

FIG. 5: The calculated total transmission coefficients $T(E)$ (which can be larger than 1) for different biases. The zero is the right electrode Fermi energy. For a given bias V, there are net right to left current flow only within the $[-V, 0]$ energy window.

After $T(E)$'s of Fig.5 are obtained, a simple energy integration between -V to 0 will give us the total current I. The resulting $I(V)$, and the conductance dI/dV are shown in Fig.6. We do see the well known peak and dip for this system in the conductance around 2V. Our calculated peak and dip positions of 1.8V and 2.3V corresponds well with the experimental results of 1.4V and 2.4V [6], and this agreement is better than previously calculated results [5]. We also see the marks of the electrode electronic structures. Near 0.3V, the conductance shows a well shape, again due to the band gaps of 2,3 bands at the X' point. Above 3.3V, we see a big drop, then the negative conductance. The drop is due to the end of the 2,3 bands at the Γ points, and the negative conductance is because the conducting electrode levels (energy window) are moving away from the conducting molecular levels. Here we see that, the electronic structure of the electrode is extremely important in determining the overall conductance of the system.

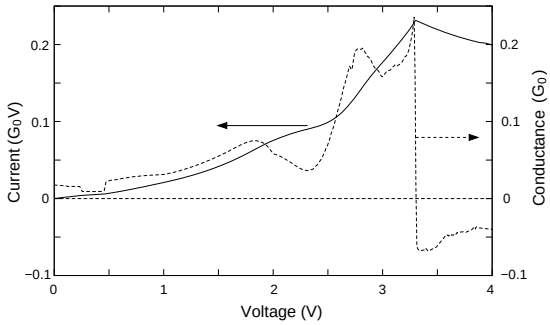

FIG. 6: The calculated I-V curve and the corresponding conductance. $G_0 = 2e/h = 77\mu s$.

In summary, we have presented a simple and numerically stable scheme to calculate the quantum transport. Within this scheme, the conventional periodic supercells and ground state ab initio programs can be used without much change. The computational effort is only a few times of a conventional ground state calculation. This promised quantum transport calculations for much larger systems which cannot be tackled by othe methods. The implementation of this method is simple and straight forward based on any conventional ground state ab initio programs.

This work was supported by U.S. Department of Energy under Contract No. DE-AC03-76SF00098. This research used the resources of the National Energy Research Scientific Computing Center.

[1] J. Taylor, H. Guo, J. Wang, Phys. Rev. B **63**, 245407 (2001); P. Damle, A. Ghosh, S. Datta, Phys. Rev. B **64**, 201403 (2001); M. B. Nardelli, J.-L. Fattebert, J. Bernholc, Phys. Rev. B **64**, 245423 (2001); M. Brandbyge, *et.al*, Phys. Rev. B **65**, 165401 (2002); E. Louis, *et.al*, Phys. Rev. B **67**, 155321 (2003).

[2] K. Hiros, M. Tsukada, Phys. Rev. B **51**, 5278 (1994);

[3] H.J. Choi, J. Ihm, Phys. Rev. B **59**, 2267 (1999).

[4] D. Z.-Y. Ting, E. T. Yu, T.C. McGillha, Phys. Rev. B **45**, 3583 (1992).

[5] M. Di Ventra, S.T. Pentelides, N. D. Lang, Phys. Rev. Lett. **84**, 979 (2000); M. Di Ventra, N. D. Lang, Phys.

Rev. B **65**, 45402 (2001).
[6] M.A. Reed, *et.al*, Science **278**, 252 (1997).
[7] C. Roland, V. Meunier, B. Larade, H. Guo, Phys. Rev. B **66**, 35332 (2002).
[8] http://crd.lbl.gov/ linwang/PEtot/PEtot.html
[9] When the energy E_i is close to an extremum of a band energy (e.g, at the Γ and X' points, or inside an anti-crossing band gap of Fig.2), an evanescent state might exist at the middle electrode cell Ω where the decomposition is calculated. These evanescent states come from the complex k-point band structure of the electrode [see: Y.C. Chang, Phys. Rev. B **25**, 605 (1982)]. If the calculated electrode is very long, these evanescent states should have decayed to zero in the middle of the electrode. But in practice, and especially when the energy is close to the extrema, these evanescent states can have significant contributions. We have used $u_n(k_m)exp(ik_m z)$ at those extrema k_m to approximate the evanescent states, and include them as $\phi_n(r)$ in the decomposition of $\phi_{i,(l)}$. Note that, these evanescent states carry no currents since $dE_n(k)/dk|_{k=k_m} = 0$.
[10] N.V. Smith, N.B. Brookes, Y. Chang, and P.D. Johnson, Phys. Rev. B **49**, 332 (1994).